THE NEW INTEGRATED CLOUD OBSERVATION CAPABILITIES OF WYOMING KING AIR BY COMBINING RADAR, LIDAR, MICROWAVE RADIOMETER AND IN SITU MEASUREMENTS

Zhien Wang, Perry Wechsler, Jeff French, Alfred Rodi, Samuel Haimov, Gabor Vali, and Dave Leon
Department of Atmospheric Science, University of Wyoming, Laramie, WY 82071

Andrew L. Pazmany
Prosensing Inc.

1. INTRODUCTION

Clouds are a critical component of the coupled earth water and energy cycles. The poor understanding of cloud-radiation-dynamics feedbacks results in large uncertainties in forecasting human-induced climate changes (Stephens, 2005; IPCC, 2007). Our current understanding of rain formation processes continues to present many challenges for weather predictions (Fritsch and Carbone, 2004). One of the greatest challenges in advancing cloud physics and model parameterizations is to provide the links involving aerosols, water vapor, cloud, precipitation, and dynamics. Continually improving our understanding of cloud physics through observations is a critical step for improving physically-based cloud microphysics parameterizations for climate and weather models. Advanced airborne cloud observational capabilities are important to achieve this goal.

Airborne in situ cloud observations have played an important role in advancing our understanding of cloud microphysical and dynamic processes by providing detailed measurements at high temporal and spatial resolutions. However, these detailed measurements are only available along a line through the cloud at flight altitude. For many physical process studies, information on the vertical structure of the cloud properties is needed. Furthermore, for many studies, interpretation of measurements from in situ probes is quite limited due to their small sampling volumes. For example, in situ cloud probes only have sampling volumes from ~40 to ~10^4 cm^3/s. The small sampling volume is an issue when studying atmospheric and cloud properties in regions with strong spatial inhomogeneities or small concentrations (such as early formation of precipitation).

Airborne remote sensing overcomes the two weaknesses of in situ sampling, although the measurements may be not as detailed as the in situ sampling. Airborne vertical profiling capabilities are mainly provided by active sensors, such as lidar and radar. Airborne radars provide unique measurements of cloud, precipitation, and cloud scale dynamics (Hildebrand et al. 1996; Heymsfield et al. 1996a; Vali et al. 1998), and have provided many insights into convective cloud systems and hurricanes (Heymsfield et al. 1996b), marine Sc clouds (Vali et al. 1998; Stevens et al. 2003; Leon et. al. 2006), and cumulus clouds (Damiani et al. 2005). Lidars operate at much shorter wavelength than radars and can provide unique measurements of cloud beyond what can be provided through radar (McGill et al. 2002). Different remote sensors, such as lidars, radars, and radiometers, respond differently to cloud particle size, concentration, and phase. For example, lidars are more sensitive to small particles and radars are more sensitive to large particles. Therefore optimally combining multiple remote sensor measurements provides potentials to improve cloud microphysical property retrievals (Wang and Sassen 2001 and 2002).

The integration of airborne in situ sampling and remote sensing provides new observational capabilities for the study of atmospheric processes and clouds. For Two-dimensional cross-sections of cloud microphysical properties retrieved from remote sensor measurements provide a context to understand detailed in situ cloud measurements. The integration of in situ and remote sensing measurements can be achieved with one or more aircraft in a field campaign. The NASA Cirrus Regional Study of Tropical Anvils and Cirrus Layers-Florida Area Cirrus Experiment (CRYSTAL-FACE, http://www.espo.nasa.gov/crystalface/index.html) in 2002 is a great example of how multiple-aircraft can be utilized effectively for interpreted integration. With two dedicated remote sensing aircraft, two in situ aircraft, and carefully coordinated flights, CRYSTAL-FACE provided a comprehensive dataset to study convectively generated anvil clouds. However, such multiple-aircraft field campaigns are very expensive to conduct. Integration of in situ and remote sensors on a single aircraft, such as reported herein, is important from an economic and logistical point of view.

Here we report on new integrated cloud observation capabilities developed for the University of Wyoming King Air (UWKA) by combining measurements from the Wyoming Cloud Lidar (WCL), a 183 GHz microwave radiometer, the Wyoming Cloud Radar (WCR) and in situ probes. The WCR has served the atmospheric community for more than 10 years and provides measures of radar reflectivity and Doppler velocity to be used to infer cloud structure and dynamics. The WCL is a newly developed compact elastic polarization lidar to provide cloud boundary as well as backscattering and depolarization ratio profiles. The radiometer provides total precipitable water vapor (PWV) and liquid water path (LWP) measurements. Combining these remote sensor measurements allows us to apply several remote sensing retrieval algorithms to better characterize the macrophysical and microphysical properties of ice, mixed-phase and water clouds. Combining in situ data and microphysical property profiles from these remote sensors provides an advanced capability to study clouds from a single aircraft. Examples are presented to illustrate this new capability.

2. INSTRUMENTATION

The UWKA is an NSF supported national, lower atmospheric observing facility and is well equipped for cloud, aerosol, and PBL studies (http://www.atmos.uwyo.edu/n2uw). The in situ and remote sensing instrumentation for cloud study is briefly discussed here.

2.1 Wyoming Cloud Radar (WCR)

The Wyoming Cloud Radar (WCR, http://www.atmos.uwyo.edu/wcr/), a 95 GHz, Doppler radar, has evolved during last 10 years. The current WCR specification is listed in Table1. It has four antennas for multiple radar beam operation (see Fig. 1). The multi-beam configuration can provide vertical and or horizontal profiles of reflectivity and Doppler velocity through clouds. The WCR has been installed in the UWKA and NCAR/NSF C-130 to study marine boundary-layer clouds, convective clouds and mixed-phase clouds.

Table 1: WCR Specifications

<table>
<tr><td>Transmit Frequency</td><td>94.92 GHz (λ=3.16 mm)</td></tr>
<tr><td>Peak Power / Max Duty Cycle</td><td>1.6 KW / 1 %</td></tr>
<tr><td>Pulse</td><td>100-500 ns</td></tr>
<tr><td>Pulse Repetition Frequency (prf)</td><td>1000 Hz – 20 KHz</td></tr>
<tr><td>Antennas:

▪ Side/Up (beam 1, use mirror for Up)
▪ Side-fore (beam 3, 36° forward)
▪ Down (beam 2, near nadir)
▪ Down-fore (beam 4, 26° forward)</td><td>4
aperture | beamwidth | polarization
0.31 m | 0.7° | H, V
0.31 m | 0.7° | single, linear
0.46 m | 0.5° | single, linear
0.38 m | 0.6° | single, linear</td></tr>
<tr><td>Antenna modes (typical):
▪ DPDD (dual-plane dual-Doppler)
▪ VPDD (vertical plane dual-Doppler)
▪ VPDD + up or side
▪ HBDD (horizontal beam dual-Doppler)
▪ HBDD+down
▪ Profiling (up+down or side+down)
▪ Profiling (up+down) + side-fore</td><td>Beams:
1,2,3,4
2,4
1,2,4
1,3
1,2,3
1,2
1,2,3</td></tr>
<tr><td>Receiver channels:
▪ receiver outputs:
▪ receiver dynamic range</td><td>2
mag: logarithmic; phase: linear
> 70 dB</td></tr>
<tr><td>Dwell time/ Along-track sampling</td><td>30 ms / 3 – 5 m (typical)</td></tr>
<tr><td>Min. detectable signal
(side-antenna , 1 StDev above mean noise)</td><td>-30 dBZ @ 1km, 250ns, 500 avrg</td></tr>
<tr><td>Resolution:
▪ range
▪ volume @ 1 km, 250 ns pulse</td><td>
15 – 75 m
37 x 12 x 15 m</td></tr>
<tr><td>Doppler velocity processor:
▪ pulse pair
▪ fft spectrum (single beam only)</td><td>
1st & 2nd moments
32 or 64 spectral lines</td></tr>
<tr><td>Max unambiguous Doppler</td><td>±15.8 m/s</td></tr>
</table>

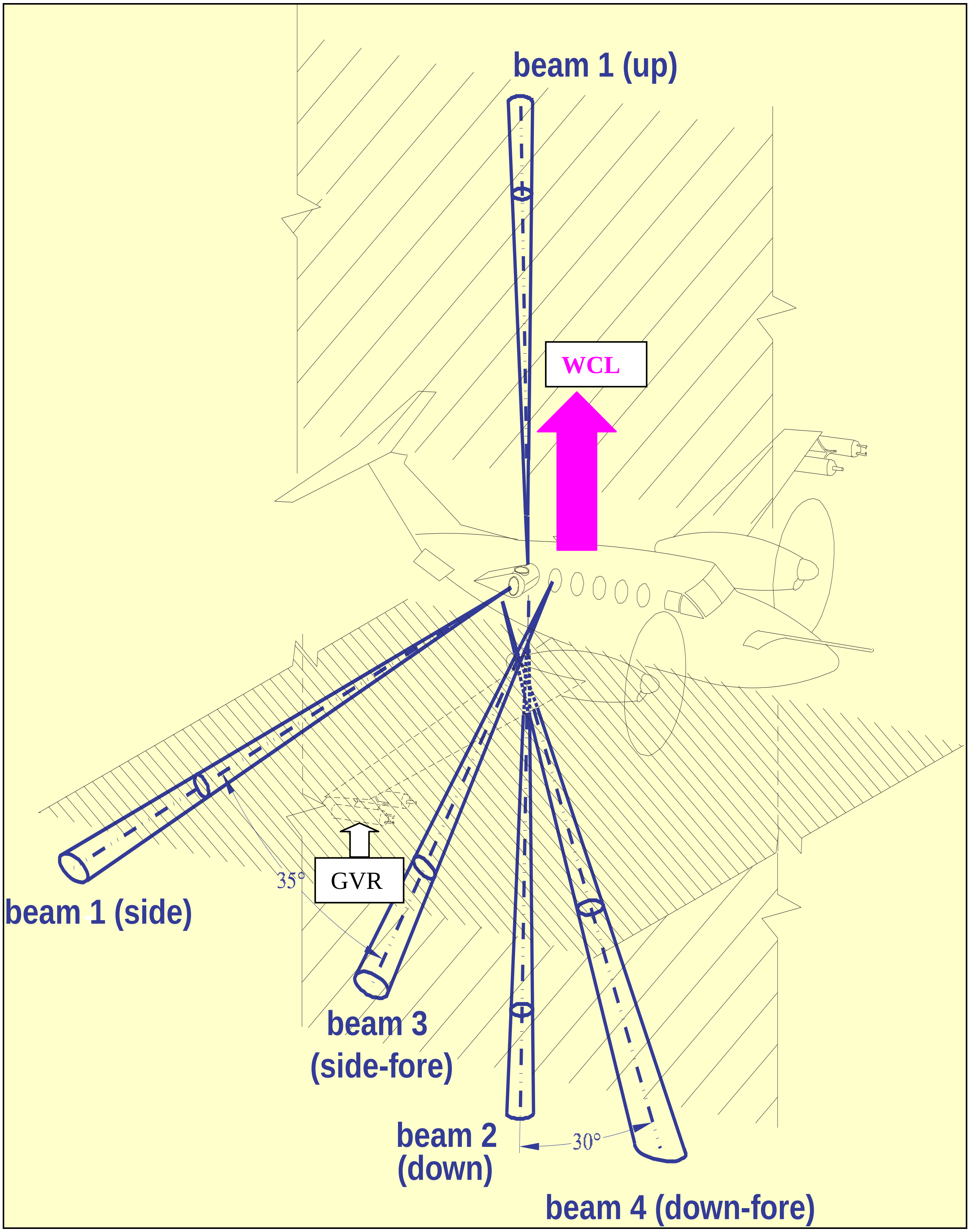

Figure 1: The beam configuration of the WCR and the installation of WCL and GVR on the Wyoming King Air.

2.2 Wyoming Cloud Lidar (WCL)

The WCL is a compact polarization lidar to provide cloud vertical structure as well as cloud particle phase information. The design goal of the WCL is to work together with the WCR to provide better cloud macrophysical and microphysical properties from UWKA or NCAR/NSF aircraft. Because of very limited space and power on the UWKA, it is not possible to simultaneously operate the WCR and a lidar with a large telescope. To use one of the existing small upward-looking ports to operate the lidar, the WCL uses a relatively high pulse-energy laser to provide the needed sensitivity. System specifications are summarized in Table 1. With the size, weight, pulse energy and eye safety of the laser in mind, the Ultra Pulsed Nd:YAG Laser from the Big Sky laser technique, Inc. is selected for the WCL. The laser provides 20 Hz 16 mJ outputs at 355 nm. The 355 nm wavelength not only provides a stronger molecular backscattering signal than other standard lidar wavelengths with the same laser energy (important for calibrating backscattering coefficients) but also eases limitations for achieving eye safe operation. The laser beam (3 mm in diameter at exit laser) is expanded 5 times before being emitted into atmosphere. This system is eye safe beyond a distance ~65 m. To improve lidar linear depolarization measurements, a ¼ λ wave plate is placed after the beam expander to work together with a cubic polarization beam splitter in the receiver path.

The laser head is integrated with transmitting and receiving optics into a compact package as the lidar head. This package is light enough to be attached to an upward-looking port on the aircraft with no additional structure. This compact design not only makes it easy to install the system on an aircraft, but also provides high mechanical stability to maintain optical alignment.

Table 2: The WCL Specification

Transmitter	
Laser Wavelength	355 nm Nd:YAG
Repetition Frequency	20 Hz
Pulse width	~8 ns
Pulse Energy	16 mJ
Receiver	
Diameter	~ 75 mm
Field of view	300 and 2000 μrad
Data System	
Number of Channels	Two
Detector	PMT
Range Resolution	3.75m, 7.5m, 15m, 30m (programmable)
Maximum Range	30 km
Data acquisition system	Combined analog and photon counting system from LICEL, GmbH

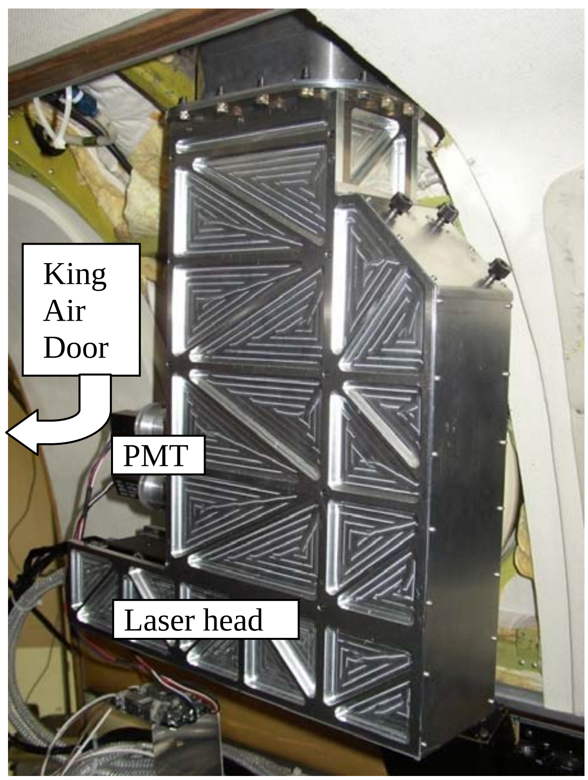

Figure 2. The WCL installation in the Wyoming King Air

2.3 Airborne 183 GHz microwave radiometer

ProSensing Inc. has developed a pod mounted G-band water Vapor Radiometer (GVR) that is mounted in a standard 2-D PMS probe canister (Pazmany 2007). Precipitable Water Vapor (PWV) and Liquid Water Path (LWP) are estimated from brightness temperatures measured in four double-sideband receiver channels, centered at 183.31 ± 1, ± 3 and ± 7, and ± 14 GHz. The airborne GVR has been installed on the CANADA NRC Convair-580 aircraft and the UWKA. The installation on UWKA is shown in Figure 3.

Because the 183 GHz water vapor absorption band is much stronger than the 23 GHz band, the GVR has better sensitivity for low PWV measurements. The 183 GHz also has stronger liquid water absorption than 31 GHz used in the traditional ground-based two-channel microwave radiometers. Thus, the GVR's high sensitivities to water vapor and liquid water make it a good microwave radiometer for airborne measurements of PWV and LWP. These column integrated quantities are important for understanding cloud system development and evolution.

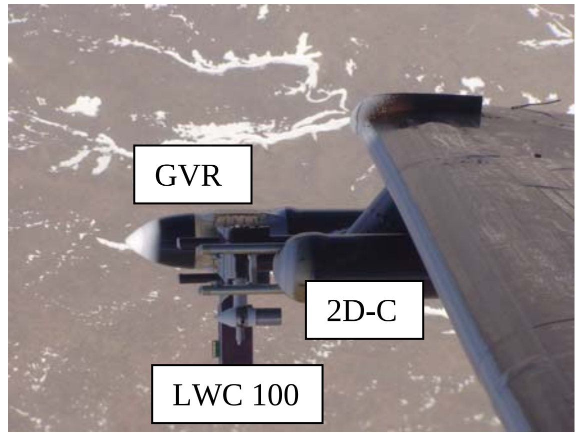

Figure 3. The GVR on the UWKA. The white cap on the GVR is the icing after penetrating a wave clouds.

2.4 In situ clouds probes

The UWKA can carry traditional in situ cloud probes (see Table 3) to provide liquid water content and hydrometer size distributions. Due to the shattering effect, the UWKA lacks capability to estimate size distributions of small ice crystals. Ice water contents (IWC) can be estimated from size distributions with factor of 2 uncertainties. Efforts are underway to upgrade the UWKA capabilities for in situ observations of ice particles.

Table 3. Current King Air in situ probes

Instrument	Measurements Available
Rosemount 871FA	Icing Rate
DMT LWC-100	Cloud Liquid Water
Gerber PVM-100	Cloud Liquid Water, Droplet Surface Area, Droplet Effective Radius
PMS FSSP-100	Cloud Particle Size Distribution (0.5 – 47μm; selectable), Total Concentration, Derived Liquid Water Content, Derived Droplet Effective Radius, Derived Droplet Surface Area, Derived Mean Volume Radius
PMS OAP-200X (1DC)	Cloud Particle Size Distribution (12.5 – 185.5 μm)
PMS OAP-2DC	Cloud Particle Images (>25 μm), Cloud Particle Size Distribution
PMS OAP-2DP	Precipitation Particle Images (>200 μm), Precipitation Particle Size Distribution

3. WYOMING AIRBORNE INTEGRATED CLOUD OBSERVATION (WAICO) EXPERIMENT

The WAICO-I experiment was conducted during February-March 2008 near Laramie, Wyoming and is supported by US National Science Foundation. The primary goal of the WAICO experiments is to develop new cloud microphysical observation capabilities by integrating the measurements of remote sensors and in situ probes.

To achieve this goal, the first task was to install the WCL, WCR, and GVR on the UWKA while carrying the full array of in situ probes. Initial challenges included staying within the allowable power budget on the UWKA. This was the first installation of the GVR on the UWKA and several technical challenges needed to be addressed before we were able to collect high quality data from this instrument. The WAICO-I successfully integrated the WCR, WCL, and GVR together with an FSSP, 2D-C and 2D-P for cloud observations. Aerosol information was provided by a Passive Cavity Aerosol Spectrometer Probe (PCASP) Model 100 and a model 3010 condensation particle counter (CPC). In addition, radiation measurements from upward- and downward-looking pyranometers (Eppley PSP, 0.285-2.8 μm), and pyrgeometers (Eppley PIR, 3.5-50 μm) were also available during the experiment.

The second task was to collect data for cloud retrieval algorithm development and validation. Based on ground-based measurements, we developed multi-sensor cloud retrieval algorithms to retrieve ice, water, and mixed-phase cloud microphysical properties (Wang and Sassen 2001 and 2002; Wang et al. 2004). The similar approaches can be applied to airborne measurements. However, the algorithms need to be modified for different combination of measurements and further validation is required. The WAICO flight patterns and target clouds were selected to collect data appropriate for both algorithm development and validation.

The third task was to collect data to study mixed-phase clouds. Compared to water and ice phase clouds, mixed-phase clouds are more complicated and are less well understood. Further, properly representing mixed-phase clouds in general circulation models (GCMs) is very important for climate simulation. Fowler et al. (1996) shows that the variation of glaciation temperatures from 0° to -40°C in a GCM simulation yields about 4 and -8 W m^{-2} differences in the top-of-atmosphere longwave and shortwave cloud radiative forcing, respectively. Other studies (Li and Le Treut 1992; Sun and Shine 1994; Gregory and Morris 1996) have shown that the treatment of mixed-phase clouds in GCMs affects either their climate sensitivity or their mean climate impact.

The integrated airborne observations developed during the WAICO provide the best observations to study mixed-phase clouds to date. The WCR is more sensitive to ice crystals than water droplets while the WCL signals are mainly dominated by water phase in the mixed-phase clouds. The LWP from GVR provide an important constraint of liquid water in the mixed-phase cloud layer. During the WAICO-I, we collected data in mixed-phase wave- and altocumulus clouds. Mixed-phase regions were also observed in deep nimbostratus clouds.

4. OBSERVATION EXAMPLES

Examples of observations from the WCR, WCL, GVR and in situ probes during the WAICO are presented in this section. The WCR provides cloud vertical structure above and below the aircraft. The WCL provides cloud structure above the aircraft. The WCL is capable of providing measurements of clouds beyond 10 m range, but the WCL signals are often saturated within 50 m. The yellow and red regions in WCL uncalibrated linear depolarization ratio indicate ice particles. The 2D-C measurements show ice crystal size distributions at flight altitude while FSSP measurements mainly show water phase properties (the red region). It is very clear that FSSP measurements are affected by large ice crystals due to the shattering effect. As illustrated in Fig. 4, LWP measurements are consistent with FSSP and lidar measurements and provide a vertical constrain on supercooled water in wave clouds above the aircraft.

4.1 wave clouds

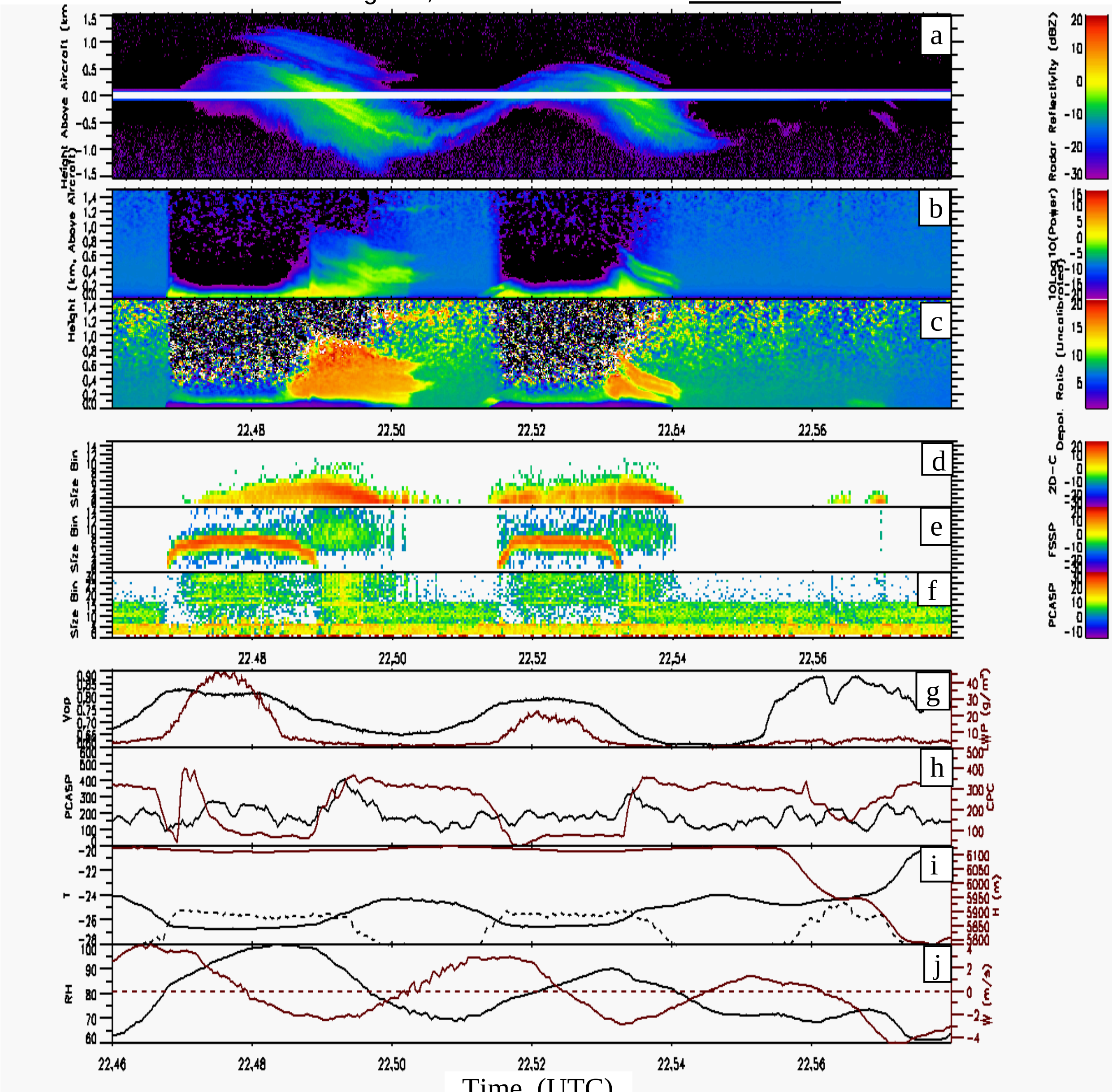

Figure 4. a) WCR radar reflectivity (the white gap indicates a zone near aircraft without measurements), b) WCL (upward pointing) returned power, c)WCL linear depolarization ratio (uncalibrated), d) 2D-C number concentration (N) for each bin (plotted as 10log(N)), e) FSSP number concentration (N) for each bin (plotted as 10log(N)), f) PCASP number concentration (N) for each bin (plotted as 10log(N)), g) Precipitable Water Vapor (Vap) and Liquid Water Path (LWP) derived from a G-band (183 GHz) water Vapor Radiometer (GVR) measurements, h) PCASP and CPC total number concentration, i) Temperature and aircraft altitude, j) RH and vertical velocity.

4.2 Optically thick ice clouds

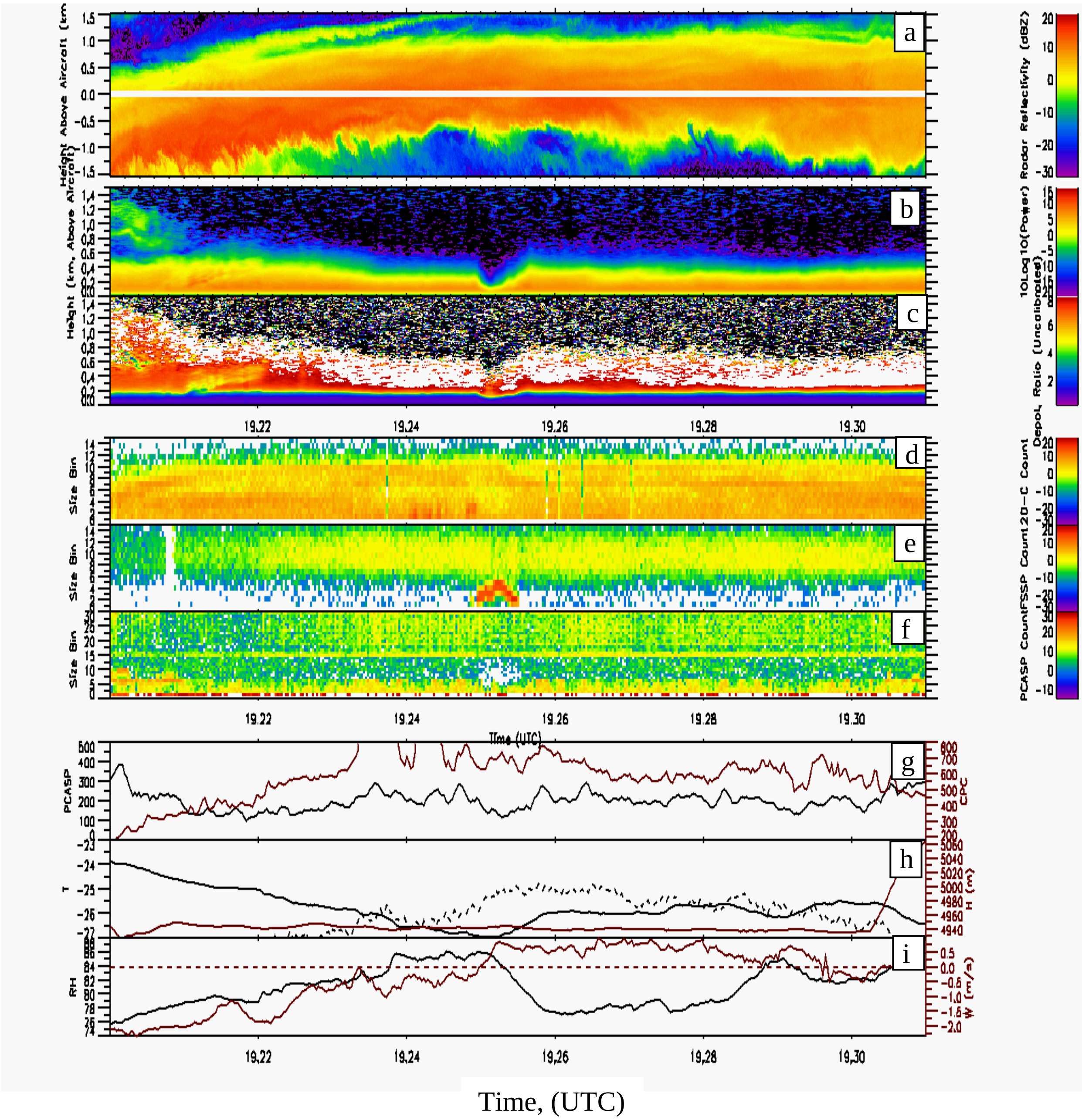

Figure 5. a) WCR radar reflectivity (the white gap indicates a zone near aircraft without measurements), b) WCL (upward pointing) returned power, c)WCL linear depolarization ratio (uncalibrated), d) 2D-C number concentration (N) for each bin (plotted as 10log(N)), e) FSSP number concentration (N) for each bin (plotted as 10log(N)), f) PCASP number concentration (N) for each bin (plotted as 10log(N)), g) PCASP and CPC total number concentration, h) Temperature and aircraft altitude, i) RH and vertical velocity.

4.3 Ice generating cell

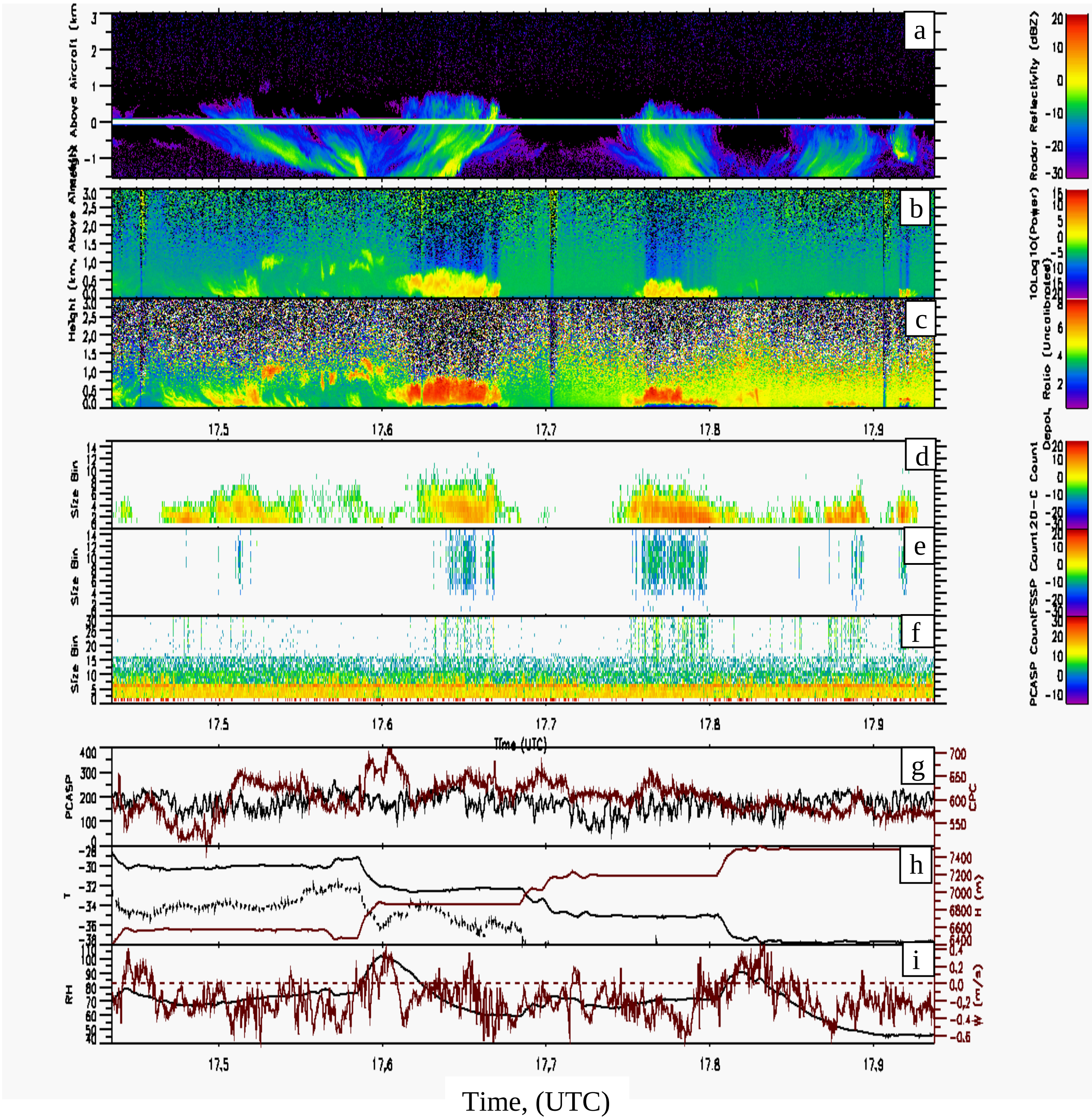

Figure 5. a) WCR radar reflectivity (the white gap indicates a zone near aircraft without measurements), b) WCL (upward pointing) returned power, c)WCL linear depolarization ratio (uncalibrated), d) 2D-C number concentration (N) for each bin (plotted as 10log(N)), e) FSSP number concentration (N) for each bin (plotted as 10log(N)), f) PCASP number concentration (N) for each bin (plotted as 10log(N)), g) PCASP and CPC total number concentration, h) Temperature and aircraft altitude, i) RH and vertical velocity.

5. CONCLUSION AND FUTURE WORK

We successfully integrated the WCR, WCL, and GVR together with a suite of in situ probes on the UWKA to observe ice and mixed-phase clouds. Combining multi-remote sensor measurements can provide cloud microphysical property vertical structures, which further provides an important context to study in situ measurements and to better understand cloud microphysical processes.

Developing algorithms to provide microphysical properties retrievals and further analysis of WAICO-I data is underway. We are planning to add a down-ward pointing lidar and test it as part of the WAICO-II campaign in spring, 2009.

With these and further planned instrumentation developments and integration and algorithm developments, we will enhance the UWKA capability to provide extended cloud microphysical and dynamic measurements for cloud study in the near future.

6. REFERENCES:

IPCC, 2007: Climate Change 2007: The Physical Science Basis. Contribution of Working Group I to the Fourth Assessment Report of the Intergovernmental Panel on Climate Change [Solomon, S., D. Qin, M. Manning, Z. Chen, M. Marquis, K.B. Averyt, M. Tignor and H.L. Miller (eds.)]. Cambridge University Press, Cambridge, United Kingdom and New York, NY, USA, 996 pp.

Damiani, R., G. Vali, and S. Haimov, 2006: The structure of thermals in cumulus from airborne dual-Doppler radar observations. *J Atmos Sci*, 1432-1450.

Fritsch, J. M., and R. E. Carbone, 2004: Improving quantitative precipitation forecasts in the warm season: A USWRP research and development strategy. *Bull. Amer. Meteor. Soc.*, **85**, 955-965.

Fowler, L. D. and D. A. Randall, 1996: Liquid and ice cloud microphysics in the CSU general circulation model .3. Sensitivity to modeling assumptions. *J Climate*, 561-586.

Gregory, D. and D. Morris, 1996: The sensitivity of climate simulations to the specification of mixed phase clouds. *Clim Dynam*, 641-651.

Heymsfield, G. M., I. J. Caylor, J. M. Shepherd, W. S. Olson, S. W. Bidwell, W. C. Boncyk, and S. Ameen, 1996a: Structure of Florida thunderstorms using high-altitude aircraft radiometer and radar observations. *J Appl Meteorol*, 1736-1762.

Heymsfield, G. M., S. W. Bidwell, I. J. Caylor, S. Ameen, S. Nicholson, W. Boncyk, L. Miller, D. Vandemark, P. E. Racette, and L. R. Dod, 1996b: The EDOP radar system on the high-altitude NASA ER-2 aircraft. *J Atmos Ocean Tech*, 795-809.

Hildebrand, P. H., W. C. Lee, C. A. Walther, C. Frush, M. Randall, E. Loew, R. Neitzel, R. Parsons, J. Testud, F. Baudin, and A. LeCornec, 1996: The ELDORA/ASTRAIA airborne Doppler Weather Radar: High-resolution observations from TOGA COARE. *B Am Meteorol Soc*, 213-232.

Li, Z. X. and H. Letreut, 1992: Cloud-Radiation feedbacks in a general circulation model and their dependence on cloud modeling assumptions. *Clim Dynam*, 133-139.

McGill, M., D. Hlavka, W. Hart, V. S. Scott, J. Spinhirne, and B. Schmid, 2002: Cloud Physics Lidar: instrument description and initial measurement results. *Appl Optics*, 3725-3734.

Pazmany, A., 2007: A Compact 183-GHz Radiometer for Water Vapor and Liquid Water Sensing. *Geoscience and Remote Sensing, IEEE Transactions on*, **45,** 2202 - 2206.

Stephens, G. L., 2005: Cloud Feedbacks in the Climate System: A Critical Review. *Journal of Climate*, **18**, 237-273.

Stevens, B., D. H. Lenschow, G. Vali, H. Gerber, A. R. Bandy, B. Blomquist, J. L.

Brenguier, C. S. Bretherton, F. Burnet, T. Campos, S. K. Chai, I. Faloona, D. Friesen, S. Haimov, K. Laursen, D. K. Lilly, S. M. Loehrer, S. P. Malinowski, B. M. Morley, M. D. Petters, D. C. Rogers, L. Russell, V. Savic-Jovac, J. R. Snider, D. Straub, M. J. Szumowski, H. Takagi, D. C. Thornton, M. Tschudi, C. Twohy, M. Wetzel, and M. C. van Zanten, 2003: Dynamics and chemistry of marine stratocumulus - Dycoms-II. *B Am Meteorol Soc*, 579-593.

Sun, Z. and K. P. Shine, 1994: Studies of the radiative properties of ice and mixed-phase clouds. *Q J R Meteorol Soc*, 111-137.

Vali, G., R. D. Kelly, J. R. French, S. Haimov, D. Leon, R. E. McIntosh, and A. Pazmany, 1998: Finescale structure and microphysics of coastal stratus. *J Atmos Sci*, 3540-3564.

Wang, Z. and K. Sassen, 2001: Cloud type and macrophysical property retrieval using multiple remote sensors. *J Appl Meteorol*, 1665-1682.

Wang, Z. and K. Sassen, 2002: Cirrus cloud microphysical property retrieval using lidar and radar measurements. Part II: Midlatitude cirrus microphysical and radiative properties. *J Atmos Sci*, 2291-2302.

Wang, Z., K. Sassen, D. Whiteman, and B. Demoz 2004: Studying altocumulus plus virga with ground-based active and passive remote sensors. *J. Appl. Meteor.,***43**, 449-460.

Acknowledgements

This research is supported by NSF under award of ATM 0645644. The Wyoming King Air is supported by NSF award ATM 0334908. The authors would like to thank the UWKA facility team involved in the WAICO experiment.